Going Beyond DTI in the Clinic: The Appeal of Microstructural MRI

Ileana Jelescu, Ph.D.

Microstructure Mapping Lab, Department of Radiology, Lausanne University Hospital (CHUV) and University of Lausanne (UNIL), Lausanne, Switzerland

Diffusion MRI has established itself as a very powerful tool to detect and quantify cellular changes in tissue. The diffusion-weighted signal is sensitized to the random displacement of water molecules in the tissue. The mean squared displacement is on the order of a few microns to tens of microns and is largely dependent on the restrictions and hindrances encountered by the water molecules in the tissue, in the form of cell membranes or other obstacles. Diffusion MRI can thus inform about tissue microstructure features that are far below the image spatial resolution – typically still 1.5 to 2.5 mm isotropic voxel size on clinical MRI systems.

Notably, since the late 1980s, diffusion MRI has been the method of choice for the diagnosis of acute stroke [1]. The dramatic drop in apparent diffusion coefficient (ADC) happening within minutes of the stroke onset is a better feature than, e.g., the increase in T2 that only occurs ~24 hours later [2]. Another clinical success story for diffusion MRI is the use of tractography in surgical or radiotherapy treatment planning [3, 4]. Tractography enables the reconstruction of white matter fibers based on the principal direction(s) of diffusion in each voxel. The underlying assumption is that diffusion along axons is much faster than perpendicular to axons, where water molecules are highly slowed down by axon membranes, myelin sheaths, and a highly tortuous extracellular space.

To account for diffusion anisotropy across the brain or other organs, the formalism of diffusion tensor imaging (DTI) was introduced early on [5]. The diffusion tensor enables reconstruction of the ADC in any arbitrary direction of space. Four scalar metrics are typically derived from the tensor: mean diffusivity (MD), fractional anisotropy (FA), axial diffusivity (AD), and radial diffusivity (RD). MD represents the average ADC across all directions of space. AD represents the diffusivity along the fastest direction of diffusion (e.g., along the white matter bundle), and RD represents the diffusivity in the radial/perpendicular plane to that. Metrics such as MD and FA have become extremely useful in the evaluation/diagnosis of many normal and pathological conditions in the brain. Outside the brain, trace-weighted images (effectively, MD) are part of clinical protocols in the liver [6–8], prostate [9], breast [10, 11], etc. The clinical value of DTI is so overwhelming that it has become a common shortcut to consider "diffusion MRI" and "DTI" as synonyms.

Here, we want to argue that the field of diffusion MRI (dMRI) is much richer than DTI, and to encourage the clinical translation and widespread adoption of more advanced dMRI protocols that enable data analysis beyond the diffusion tensor. The compatibility of protocols with the clinic is largely driven by scan time and by feasibility across scanners and imaging centers. Recent technological advances now enable the acquisition of more comprehensive dMRI data than DTI in a clinically feasible scan time (< 10 min) [12]. These advances concern MRI scanner hardware and notably stronger gradients, acquisition acceleration techniques such as GRAPPA [13] or multiband [14], and processing strategies that boost data quality, such as denoising [15, 16].

What is the advantage of acquiring richer data than is needed for the DTI estimation? And what is meant by "richer data"? DTI assumes that the diffusion signature in any voxel can be modeled as an ellipsoid. This is commonly referred to as the "Gaussian Phase Approximation", which holds up to a moderate diffusion weighting of b ~1000 s/mm^2 in vivo[1] (Fig. 1). However, biological tissue contained in a voxel is in fact complex and heterogeneous. There is significant value in retrieving specific information about features such as cellular density, morphology, characteristic sizes, myelination, etc. This is the challenge that the field of microstructural MRI has taken on, with remarkable progress and success stories over the past few years [12, 17–19].

[1] *Please note that the Gaussian Phase Approximation does not imply isotropy. A medium can be Gaussian anisotropic.*

Beyond DTI: Diffusion kurtosis imaging

Firstly, sensitivity to tissue complexity and heterogeneity can already be gleaned from the behavior of the diffusion-weighted signal beyond the Gaussian Phase Approximation, i.e., for b-values > 1000 s/mm². This heterogeneity is measured by the "kurtosis" (Fig. 1). Diffusion Kurtosis Imaging (DKI) is thus a clinically feasible extension of DTI that estimates the kurtosis tensor jointly with the diffusion tensor [21]. Summary metrics derived from the kurtosis tensor are mean, axial, and radial kurtosis (MK, AK, RK). Qualitatively, high kurtosis suggests high diffusion heterogeneity in the voxel, or microstructural complexity. For example, radial kurtosis is high in aligned white matter fiber bundles, due to the two very different water populations – highly restricted in the intra-axonal space and more mobile in the extra-axonal space. Demyelination, axonal loss, or membrane permeation will reduce kurtosis. Inflammation on the other hand can increase kurtosis due to increased cellularity [20]. While diffusivity and kurtosis typically change in opposite directions with physiological and pathological processes (i.e., kurtosis decreases when diffusivity increases), numerous studies have shown DKI to provide complementary information to DTI about tissue microstructure. For example, in voxel-based or ROI-based analyses, kurtosis metrics can identify differences between patients and controls in brain regions where DTI metrics do not (Fig. 2). DKI is thus used to improve the detection of brain changes during, for instance, development [22, 23], aging [24], early psychosis and schizophrenia [25–27], cognitive impairment and Alzheimer's disease [28], multiple sclerosis [29], glioma [30], stroke [31, 32], traumatic brain injury [33, 34], and prostate and other body applications [35]. While DTI estimation can be done using typically ~30 directions of a single non-zero b-value referred to as a "shell" (usually b = 1000 s/mm²), two non-zero shells are needed for DKI estimation. A typical DKI protocol would thus include an additional b = 2000–2500 s/mm² shell with ~30 directions. It is critical that the entire protocol (b = 0, 1000, 2000) is set up as a single scan, such that the echo time (TE) is consistent across all diffusion-weighted images. Data compatible with the DKI estimation can

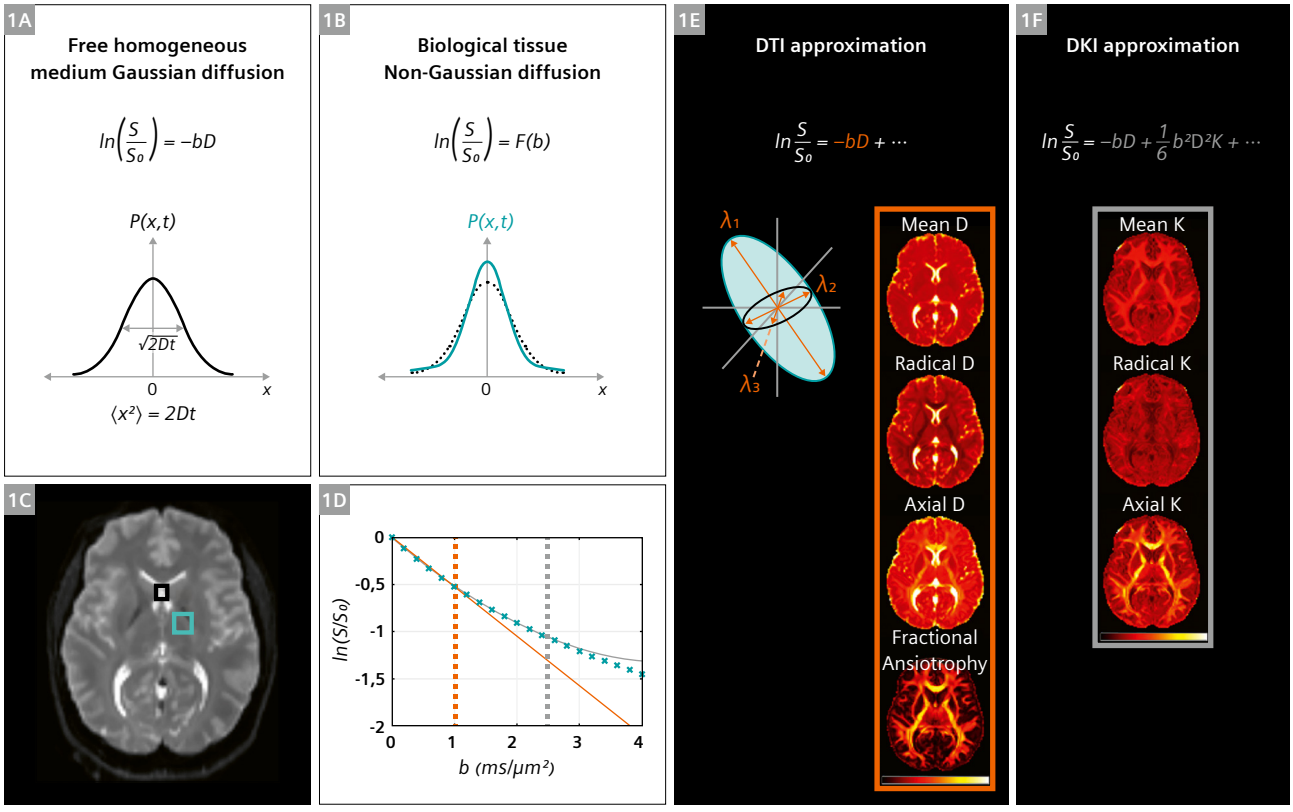

1 **(1A)** In a free homogeneous medium, such as cerebrospinal fluid (black box in (1C)), the displacement probability follows a Gaussian shape, whereby the diffusion process is referred to as Gaussian. **(1B)** In biological tissue, such as brain white matter (petrol box in (1C)), the displacement probability is no longer Gaussian; it is more peaked (positive kurtosis). **(1D)** The diffusion-weighted MRI signal (petrol) can be approximated as Gaussian (orange solid line, DTI) only up to a low b-value (~1 ms/μm² or 1000 s/mm², orange dashed vertical line), after which it deviates from a linear pattern and can be described by a quadratic function (gray solid line, DKI) up to moderate b-value (~2.5 ms/μm² or 2500 s/mm², gray dashed vertical line). Corresponding parametric maps are shown in **(1E)** for DTI and **(1F)** for DKI metrics of a 33-year-old female. Diffusivities scale bar: [0 3] μm²/ms, FA [0 1], and kurtosis [0 3]. *Figure adapted from [20], with permission.*

currently be acquired in a scan time of 6–7 minutes, at a resolution of 2 mm isotropic.

The availability of two-shell (or even better, multi-shell) dMRI data really boosts the number of analyses that the data are suitable for, as compared to single-shell. Aside from enabling DKI estimation, two or more shells also improve the estimation of the orientation distribution function (ODF) at every voxel, in order to refine tractography reconstructions [36, 37] and especially to make the data suitable for estimating biophysical models of diffusion, which are at the heart of microstructural MRI.

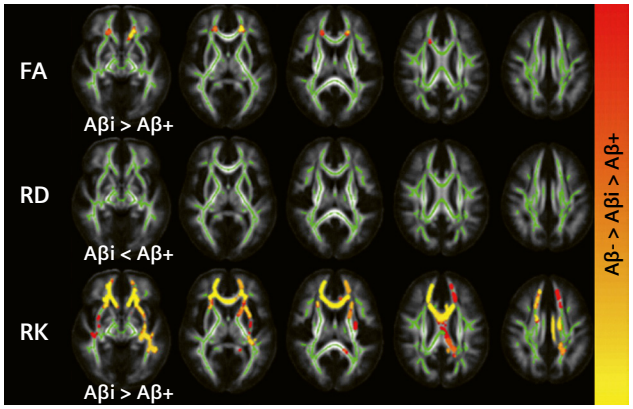

2 Axial views show significant differences between patients with intermediate beta-amyloid levels (Aβi) and amyloid-positive patients (Aβ+) for FA, RD, and RK. Significantly reduced RK in Aβ+ as compared to Aβi is more widespread in the brain than reduced FA or increased RD. *Figure adapted from [28], with permission.*

Indeed, the metrics provided by DTI and DKI analyses – MD, FA, and MK – are sensitive to physiological and pathological processes, but they lack specificity in the sense that various processes can yield the same signature in terms of these diffusion metrics. For example, a decrease in FA in white matter can be caused by mechanisms as varied as demyelination, axonal loss, microgliosis, etc. [38]. To retrieve specificity, biophysical models of diffusion in a given tissue type are introduced.

Brain white matter

The most popular and studied model is certainly the two- or three-compartment model of diffusion in white matter (Fig. 3). Here, one compartment represents the collection of axons, and the second compartment represents the extra-axonal space. The two-compartment model of diffusion in white matter thus captures five parameters [f, $D_{i,\parallel}$, $D_{e,\parallel}$, $D_{e,\perp}$, p_2], which can all be estimated independently using a two-shell acquisition similar to the DKI scheme. Each one has its own microstructural relevance and improves the specific characterization of white matter pathology, as summarized in Figure 3 and supported by several preclinical and human validation studies [20, 39–44].

A third compartment can sometimes be used to capture the cerebrospinal fluid (CSF) partial volume as a sixth parameter, with the additional f_{iso} for CSF fraction. However, recent evidence suggests that estimating the

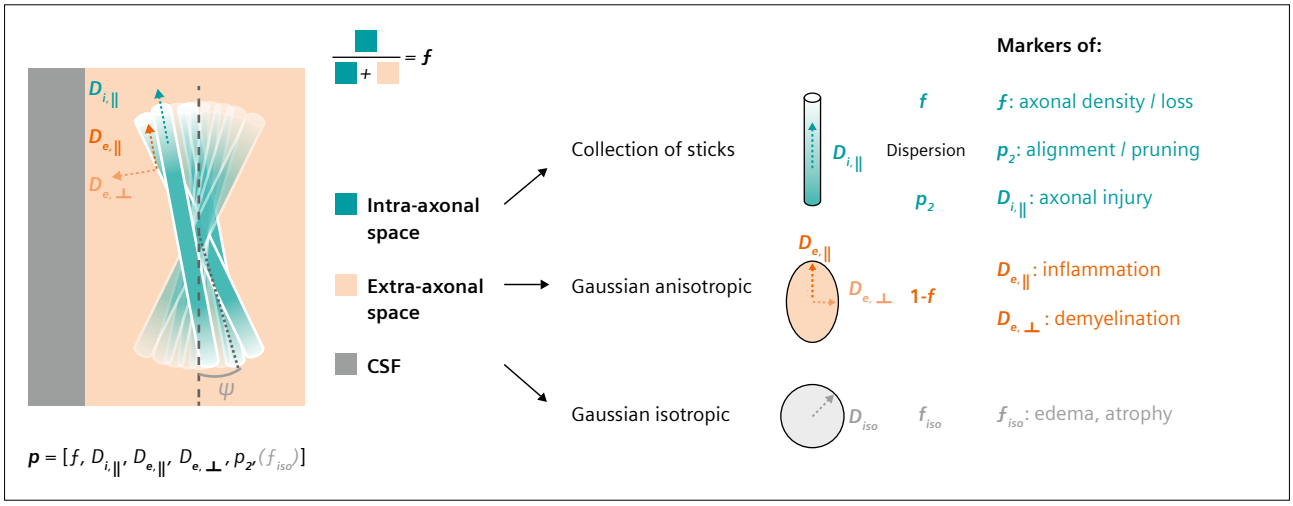

3 The Standard Model of diffusion in white matter. Axons are modeled as a collection of infinitely long sticks (cylinders with zero radius), where diffusion is unidirectional with diffusivity $D_{i,\parallel}$. They occupy a relative voxel water fraction f and their orientation distribution function (ODF) can be parametrized using an expansion in spherical harmonic coefficients; in practice, only the first coefficient p_2 is usually estimated, which gives a measurement of orientation dispersion (ranging between $p_2 = 0$ for isotropically distributed axons and $p_2 = 1$ for perfectly aligned axons). Extra-axonal water is modeled as a Gaussian anisotropic medium with diffusivities $D_{e,\parallel}$ and $D_{e,\perp}$ in the parallel and perpendicular directions, respectively. A third possible compartment is CSF, which is modeled as a Gaussian isotropic medium with fixed diffusivity $D_{iso} = 3\ \mu m^2/ms$ (the diffusivity of free water at body temperature), occupying a relative voxel water fraction f_{iso}. In this case, the fractions are normalized such that they add up to 1: $S_{tot} = (1 - f_{iso})(f \cdot S_{intra} + (1 - f) \cdot S_{extra}) + f_{iso} \cdot S_{CSF}$.

three-compartment model requires data beyond single-TE and linear diffusion encoding schemes to be robust [45].

We thus consider the two-compartment model of white matter to be compatible with clinical protocols. The estimation of the five parameters requires at least two shells with b-values (1000/2000) s/mm² sampled across at least 30 directions. Several implementations of this model have been proposed over the years using various acronyms, including NODDI [46], WMTI [47], WMTI-Watson [48, 49], and CHARMED [50]. However, they can all be unified under a Standard Model [51], which can be estimated using a choice of publicly available software tools: [45, 48] (Fig. 4). Importantly, these recommended implementations of the Standard Model estimation do not fix any parameters to arbitrary values to stabilize the fit. This maintains a high specificity of each parameter to its biological description. Indeed, pathology can, for example, alter compartment diffusivities (e.g., $D_{e,\parallel}$ decreases due to axonal injury [52]), an effect which can only be captured if $D_{e,\parallel}$ is a free model parameter. If it is fixed to an arbitrary value, the pathological change will be incorrectly absorbed by another parameter of the model [53].

The value of white matter microstructure characterization using the Standard Model vs. DTI has been demonstrated in several studies of clinical populations, and notably at early stages of change, such as in mild cognitive impairment, early psychosis, acute ischemia, multiple sclerosis, and early brain development [27, 28, 54]. For example, the Standard Model reveals mainly a decrease in axonal water fraction and an increase in extra-axonal diffusivities in early psychosis compared to controls, pointing to an extra-axonal-initiated pathology possibly with myelin damage [27]. The model reveals a decrease in axonal water fraction and in intra-axonal diffusivity in cognitive impairment, pointing to an intra-axonal-initiated pathology [28, 52]. Unfortunately, the model cannot be applied retrospectively to single-shell clinical data, despite what some implementations suggest [55]. Its broader use thus warrants a change in default diffusion clinical protocol from the single-shell DTI to two or three shells. We underline once more that the cost in scan time remains very moderate thanks to acceleration techniques, and is superseded by the benefits of a more refined white matter characterization.

Brain gray matter

Modeling diffusion in gray matter is more challenging than in white matter: The limited myelination does not guarantee that water will stay within the same compartment over typical clinical diffusion times ($\Delta > 20$ ms) and thus inter-compartment water exchange must be modeled. A recent model suitable for cortical gray matter has been proposed: Neurite EXchange Imaging (NEXI)[2]. It has been successfully demonstrated and validated, first on preclinical MRI systems [56, 57], then on Connectom scanners from Siemens Healthineers [58, 59] and recently also on a 3T MAGNETOM Prisma system from Siemens Healthineers

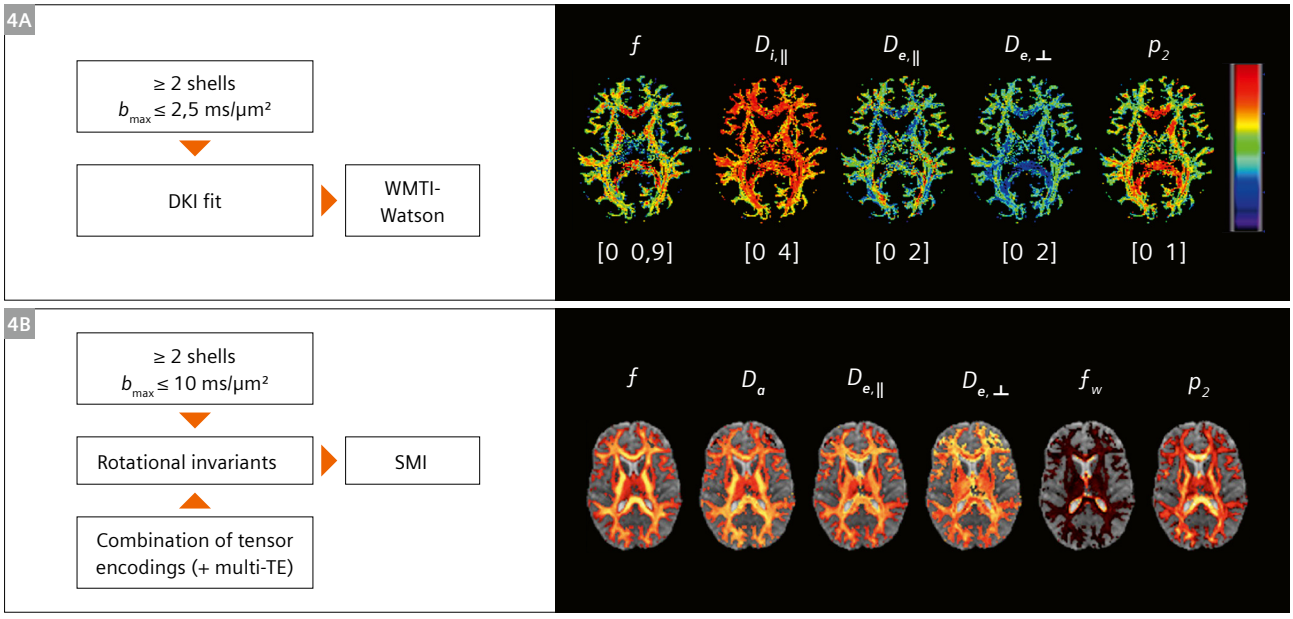

4 **(4A)** The WMTI-Watson implementation of the Standard Model can be estimated directly from a DKI fit using, for example, a deep-learning implementation in [48] available at https://github.com/Mic-map/WMTI-Watson_DL. **(4B)** The Standard Model Imaging (SMI) toolbox is suitable for both classical DKI data (2 shells, b_{max} up to 2500 s/mm²) as in **(4A)** or richer data such as multi-shell up to b_{max} = 10,000 s/mm² and/or combinations of measurements using linear and spherical diffusion encoding or multi-TE [45]. The toolbox is available at https://github.com/NYU-DiffusionMRI/SMI. *SMI maps adapted from [45], with permission.*

[60, 61] (Fig. 5). Briefly, NEXI is a two-compartment model that disentangles contributions from intra-neurite water and extra-neurite water and estimates the exchange time t_{ex} across the cellular membrane. Accounting for the exchange enables a more accurate estimation of neurite density (which would be otherwise underestimated), while the measurement of the exchange time itself is a relevant proxy for cell membrane integrity and gray matter myelination [56, 62]. The biomarker value of NEXI parameters remains to be thoroughly validated, though initial preclinical and clinical studies are encouraging [56, 60, 63].

However, the estimation of NEXI model parameters requires a diffusion protocol that can only be set up using research applications. Indeed, it requires sampling both dimensions of (q, t) space independently, as opposed to aggregated within the b-value.[3] In other words, the diffusion time t needs to be controlled directly in the sequence card, an option which is currently not available in the diffusion product sequences from Siemens Healthineers. NEXI is for now mainly suitable for research protocols, but it holds great promise for characterizing gray matter pathology in patient cohorts. This model could be extended to also account for cell bodies, which are more abundant in gray than white matter, but the feasibility of estimating all model parameters reliably is under investigation [57].

Beyond the brain: tumors, prostate, muscle

Moving away from the brain, biophysical models of diffusion MRI have been developed for other tissue types and organs. However, to unleash the potential of microstructural MRI for non-brain applications, advanced dMRI protocols also must be established prospectively.

Certainly, the reliable estimation of diffusion models outside the brain also requires data acquisition beyond what is typically feasible with the diffusion product sequence. Protocols need to span multiple diffusion times, and often also beyond the pulsed-gradient spin-echo (PGSE) scheme, using either OGSE (Oscillating-Gradient Spin-Echo)[4] [64] or STEAM (Stimulated Echo)[4] [65].

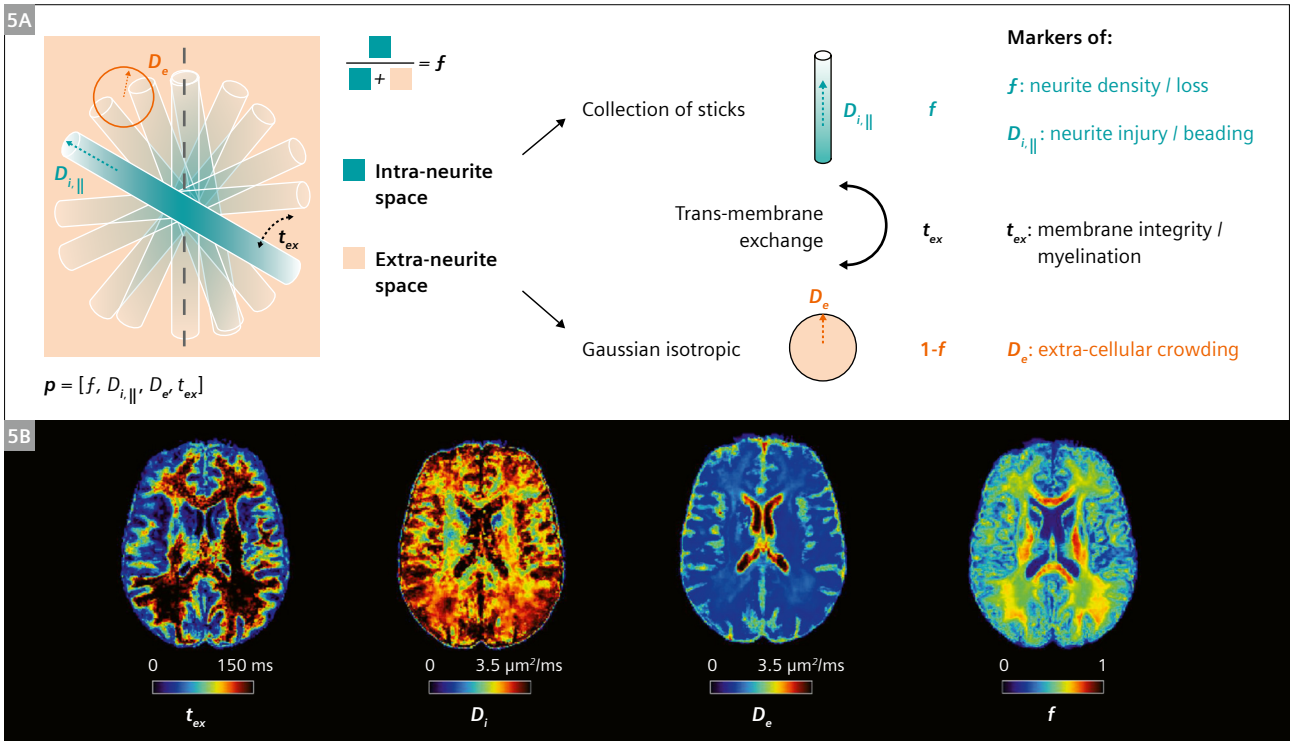

5 **(5A)**: NEXI is a two-compartment model capturing four parameters: the intra-neurite water fraction f, the intra-neurite diffusivity D_i (where neurites are modeled as infinitely long sticks, randomly oriented), the extra-cellular diffusivity D_e, assumed isotropic, and the water exchange time t_{ex} between the intracellular and extracellular compartments. **(5B)**: Example NEXI maps in the human brain. *Adapted from [59], with permission.* NEXI can be estimated using publicly available code: https://github.com/Mic-map/nexi.

[2]Siemens Healthineers Disclaimer: This article describes possible future ideas and concepts. It is not intended to describe specific performance and/or safety characteristics of currently planned or future products. Future realization and availability cannot be guaranteed.

[3]For the pulsed-gradient spin-echo (PGSE) diffusion weighting, and in the narrow pulse approximation: $b = (\gamma G\delta)^2 (\Delta - \delta/3) = q^2 t$, where q is the spatial phase warp and t is the diffusion time.

[4]The product is still under development and not commercially available. Its future availability cannot be ensured.

Compared to PGSE, OGSE and STEAM acquisitions give access to diffusion times that are much shorter or longer, respectively. These diffusion encoding schemes are available as part of research protocols. Beyond linear diffusion encoding (i.e., sensitizing the signal to diffusion along one specific direction at a time), diffusion gradient waveforms tailored to enable multi-dimensional diffusion encoding are sometimes also required [66]. They are available through C2P (https://github.com/filip-szczepankiewicz/fwf_seq_resources/tree/master/Siemens).

Tumors are a perfect application for microstructural MRI. Their heterogeneity is difficult to capture with DTI metrics alone. Usually, the tumor environment is modelled as impermeable spheres of a given radius within an extracellular space. Cell size can then be estimated through varying diffusion times, using PGSE or a combination of PGSE and OGSE measurements, depending on the time range that needs to be sampled. Two common models are IMPULSED (Imaging Microstructural Parameters Using Limited Spectrally Edited Diffusion) [67] and POMACE (Pulsed and Oscillating gradient MRI for Assessment of Cell size and Extracellular space) [68]. Several clinical studies have successfully exploited diffusion time-dependence to characterize glioma [69, 70] or prostate cancer [71]. Using multi-dimensional diffusion encoding, it is possible to also probe the shapes of the cells that constitute the tumor. Consider a voxel of spherical cell bodies vs. a voxel of isotropically oriented neurites. Both scenarios would yield similar diffusion signatures in single diffusion encoding (PGSE or OGSE) methods – e.g., a very low FA in both cases. Multi-dimensional diffusion encoding enables separating these two cases by extracting the "microscopic FA" (μFA), which would be very low for spherical cells and very high for neurites and astrocytic processes (Fig. 6). One approach to multiple diffusion encoding is *q*-space trajectory imaging, or diffusion tensor (b-tensor) encoding, which consists in using time-varying ("free") diffusion gradient waveforms to probe multiple directions at once [73, 74]. One of its most successful applications was in discriminating between various types of tumors characterized by different cell geometries [72, 75, 76] (Fig. 6). It has also been used to assess kidney microstructure [77] and to improve the estimation of the Standard Model of white matter [45].

The reader is referred to dedicated reviews on tumor microstructure characterization [76, 78, 79].

In the case of prostate microstructure, the model accounts for a densely packed cellular compartment (composed of stroma and epithelium), for which the fiber diameter and membrane permeability can be estimated using the random permeable barrier model (RPBM), and a luminal compartment with almost unrestricted water diffusion, for which the average lumen diameter can be estimated. The model therefore requires an acquisition where the diffusion time is varied using a STEAM scheme, and the echo time TE is also varied to separate water pools with different T2s [80]. This model has been successfully applied to the characterization of healthy and cancerous

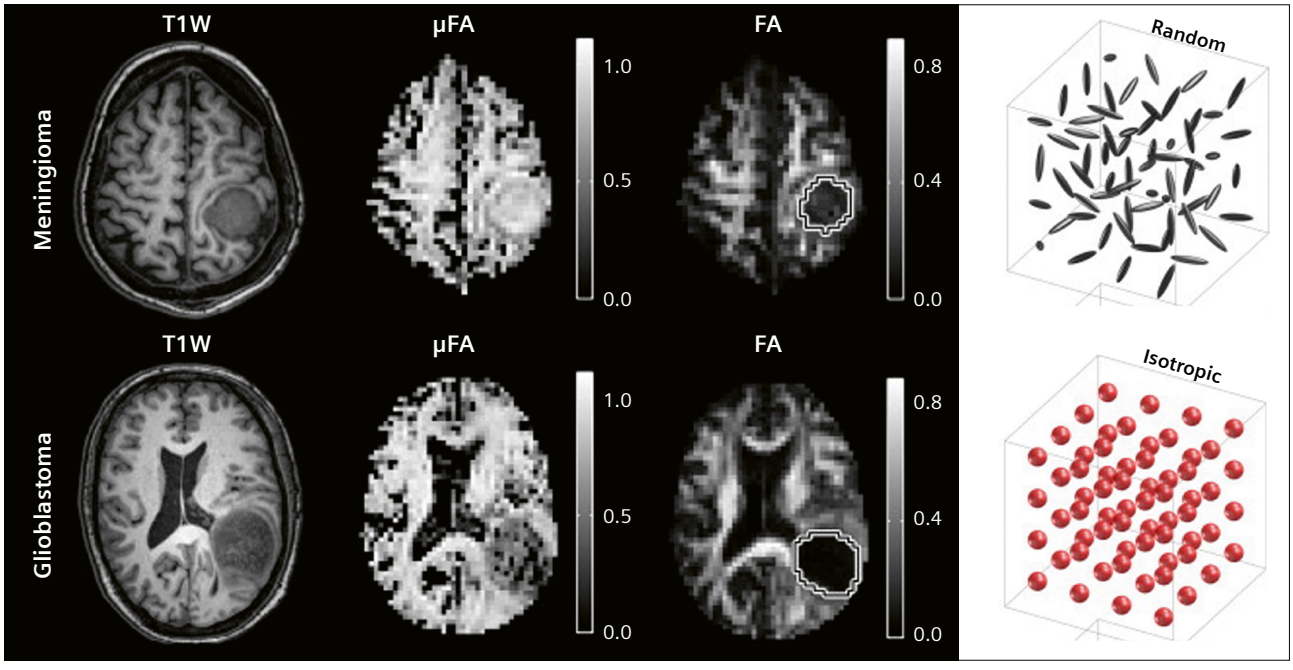

6 A meningioma (top row) and glioblastoma (bottom row) display similar contrast on T1w images and low FA. However, the μFA estimated from a combined acquisition of linear and spherical diffusion encoding is high in the meningioma and low in the glioblastoma. This is due to their underlying most abundant microstructure (sketched in the right-hand column). *Figure adapted from [86], with permission.*

prostate [81] with the potential of eventually foregoing the need for invasive biopsies.

Finally, time-dependent diffusion MRI also serves microstructural quantification of skeletal muscle. The RPBM model has been applied to estimate myofiber diameter changes due to injury-related atrophy and subsequent recovery [82]. Recently, clinical applications of time-dependent diffusion to Duchenne muscular dystrophy have also been performed [83].

Conclusion and future directions

The diffusion MRI signal contains very valuable information about tissue microstructure, and the regime that goes beyond the Gaussian Phase Approximation and DTI enables a more refined and specific characterization of cellular-level features. It is worthwhile acquiring multi-shell data routinely in clinical practice to improve sensitivity and specificity to pathology. We also encourage the widespread adoption of more advanced research protocols, which may include varying the diffusion time and/or the dimensionality of diffusion encoding, and which are particularly useful for brain gray matter and body imaging. A community-wide reflection on how to best integrate quantitative microstructure maps into the clinical workflow is much needed for radiologists and clinicians to make use of the available information. For example, normative databases for diffusion microstructure parameters like the ones developed for relaxometry [84] are currently in development [85]. They would enable evaluating the extent of alterations on a patient-by-patient basis.

References

1 Moseley ME, de Crespigny AJ, Roberts TP, Kozniewska E, Kucharczyk J. Early detection of regional cerebral ischemia using high-speed MRI. Stroke. 1993;24(12 Suppl):I60–5.
2 Lansberg MG, Thijs VN, O'Brien MW, Ali JO, de Crespigny AJ, Tong DC, et al. Evolution of apparent diffusion coefficient, diffusion-weighted, and T2-weighted signal intensity of acute stroke. AJNR Am J Neuroradiol. 2001;22(4):637–644.
3 Panesar SS, Abhinav K, Yeh FC, Jacquesson T, Collins M, Fernandez-Miranda J. Tractography for Surgical Neuro-Oncology Planning: Towards a Gold Standard. Neurotherapeutics. 2019;16(1):36–51.
4 Shahbandi A, Sattari SA, Haghshomar M, Shab-Bidar S, Lawton MT. Application of diffusion tensor-based tractography in treatment of brain arteriovenous malformations: a systematic review. Neurosurg Rev. 2023;46(1):115.
5 Basser PJ, Mattiello J, LeBihan D. Estimation of the effective self-diffusion tensor from the NMR spin echo. J Magn Reson B. 1994;103(3):247–254.
6 Chandarana H, Taouli B. Diffusion and perfusion imaging of the liver. Eur J Radiol. 2010;76(3):348–358.
7 Girardet R, Dubois M, Manasseh G, Jreige M, Du Pasquier C, Canniff E, et al. The combination of non-contrast abbreviated MRI and alpha foetoprotein has high performance for hepatocellular carcinoma screening. Eur Radiol. 2023;33(10):6929–6938.
8 Sobeh T, Inbar Y, Apter S, Soffer S, Anteby R, Kraus M, et al. Diffusion-weighted MRI for predicting and assessing treatment response of liver metastases from CRC – A systematic review and meta-analysis. Eur J Radiol. 2023;163:110810.
9 Padhani AR, Schoots IG. Prostate cancer screening-stepping forward with MRI. Eur Radiol. 2023;33(10):6670–6676.
10 Iima M, Honda M, Sigmund EE, Ohno Kishimoto A, Kataoka M, Togashi K. Diffusion MRI of the breast: Current status and future directions. J Magn Reson Imaging. 2020;52(1):70–90.
11 Partridge SC, Nissan N, Rahbar H, Kitsch AE, Sigmund EE. Diffusion-weighted breast MRI: Clinical applications and emerging techniques. J Magn Reson Imaging. 2017;45(2):337-355.
12 Jelescu IO, Palombo M, Bagnato F, Schilling KG. Challenges for biophysical modeling of microstructure. J Neurosci Methods. 2020;344:108861.
13 Griswold MA, Jakob PM, Heidemann RM, Nittka M, Jellus V, Wang J, et al. Generalized autocalibrating partially parallel acquisitions (GRAPPA). Magn Reson Med. 2002;47(6):1202–1210.
14 Feinberg DA, Setsompop K. Ultra-fast MRI of the human brain with simultaneous multi-slice imaging. J Magn Reson. 2013;229:90–100.
15 Moeller S, Pisharady PK, Ramanna S, Lenglet C, Wu X, Dowdle L, et al. NOise reduction with DIstribution Corrected (NORDIC) PCA in dMRI with complex-valued parameter-free locally low-rank processing. Neuroimage. 2021;226:117539.
16 Veraart J, Novikov DS, Christiaens D, Ades-Aron B, Sijbers J, Fieremans E. Denoising of diffusion MRI using random matrix theory. Neuroimage. 2016;142:394–406.
17 Alexander DC, Dyrby TB, Nilsson M, Zhang H. Imaging brain microstructure with diffusion MRI: practicality and applications. NMR Biomed. 2019;32(4):e3841.
18 Novikov DS, Fieremans E, Jespersen SN, Kiselev VG. Quantifying brain microstructure with diffusion MRI: Theory and parameter estimation. NMR Biomed. 2019;32(4):e3998.
19 Novikov DS, Kiselev VG, Jespersen SN. On modeling. Magn Reson Med. 2018;79(6):3172–3193.
20 Jelescu IO, Fieremans E. Chapter 2 - Sensitivity and specificity of diffusion MRI to neuroinflammatory processes. In: Laule C, Port JD (Eds.). Advances in Magnetic Resonance Technology and Applications. Imaging Neuroinflammation. Academic Press. 2023:31–50. https://doi.org/10.1016/B978-0-323-91771-1.00010-1
21 Jensen JH, Helpern JA, Ramani A, Lu H, Kaczynski K. Diffusional kurtosis imaging: the quantification of non-gaussian water diffusion by means of magnetic resonance imaging. Magn Reson Med. 2005;53(6):1432–1440.
22 Jelescu IO, Veraart J, Adisetiyo V, Milla SS, Novikov DS, Fieremans E. One diffusion acquisition and different white matter models: how does microstructure change in human early development based on WMTI and NODDI? Neuroimage. 2015;107:242–256.
23 Paydar A, Fieremans E, Nwankwo JI, Lazar M, Sheth HD, Adisetiyo V, et al. Diffusional kurtosis imaging of the developing brain. AJNR Am J Neuroradiol. 2014;35(4):808–814.
24 Benitez A, Jensen JH, Falangola MF, Nietert PJ, Helpern JA. Modeling white matter tract integrity in aging with diffusional kurtosis imaging. Neurobiol Aging. 2018;70:265–275.
25 Cho KIK, Kwak YB, Hwang WJ, Lee J, Kim M, Lee TY, et al. Microstructural Changes in Higher-Order Nuclei of the Thalamus in Patients With First-Episode Psychosis. Biol Psychiatry. 2019;85(1):70–78.
26 Kochunov P, Rowland LM, Fieremans E, Veraart J, Jahanshad N, Eskandar G, et al. Diffusion-weighted imaging uncovers likely sources of processing-speed deficits in schizophrenia. Proc Natl Acad Sci U S A. 2016;113(47):13504–13509.

27 Pavan T, Alemán-Gómez Y, Jenni R, Steullet P, Schilliger Z, Dwir D, et al. White Matter Microstructure Alterations and Their Link to Symptomatology in Early Psychosis and Schizophrenia. 2024. https://doi.org/10.1101/2024.02.01.24301979

28 Dong JW, Jelescu IO, Ades-Aron B, Novikov DS, Friedman K, Babb JS, et al. Diffusion MRI biomarkers of white matter microstructure vary nonmonotonically with increasing cerebral amyloid deposition. Neurobiol Aging. 2020;89:118–128.

29 de Kouchkovsky I, Fieremans E, Fleysher L, Herbert J, Grossman RI, Inglese M. Quantification of normal-appearing white matter tract integrity in multiple sclerosis: a diffusion kurtosis imaging study. J Neurol. 2016;263(6):1146–1155.

30 Bai Y, Lin Y, Tian J, Shi D, Cheng J, Haacke EM, et al. Grading of Gliomas by Using Monoexponential, Biexponential, and Stretched Exponential Diffusion-weighted MR Imaging and Diffusion Kurtosis MR Imaging. Radiology. 2016;278(2):496–504.

31 Hui ES, Fieremans E, Jensen JH, Tabesh A, Feng W, Bonilha L, et al. Stroke assessment with diffusional kurtosis imaging. Stroke. 2012;43(11):2968–2273.

32 Umesh Rudrapatna S, Wieloch T, Beirup K, Ruscher K, Mol W, Yanev P, et al. Can diffusion kurtosis imaging improve the sensitivity and specificity of detecting microstructural alterations in brain tissue chronically after experimental stroke? Comparisons with diffusion tensor imaging and histology. Neuroimage. 2014;97:363–373.

33 Chen J, Chung S, Li T, Fieremans E, Novikov DS, Wang Y, et al. Identifying relevant diffusion MRI microstructure biomarkers relating to exposure to repeated head impacts in contact sport athletes. Neuroradiol J. 2023;36(6):693–701.

34 Karlsen RH, Einarsen C, Moe HK, Håberg AK, Vik A, Skandsen T, et al. Diffusion kurtosis imaging in mild traumatic brain injury and postconcussional syndrome. J Neurosci Res. 2019;97(5):568–581.

35 Rosenkrantz AB, Padhani AR, Chenevert TL, Koh DM, De Keyzer F, Taouli B, et al. Body diffusion kurtosis imaging: Basic principles, applications, and considerations for clinical practice. J Magn Reson Imaging. 2015;42(5):1190–1202.

36 Guo F, Leemans A, Viergever MA, Dell'Acqua F, De Luca A. Generalized Richardson-Lucy (GRL) for analyzing multi-shell diffusion MRI data. Neuroimage. 2020;218:116948.

37 Jeurissen B, Tournier JD, Dhollander T, Connelly A, Sijbers J. Multi-tissue constrained spherical deconvolution for improved analysis of multi-shell diffusion MRI data. Neuroimage. 2014;103:411–426.

38 Jelescu IO, Budde MD. Design and validation of diffusion MRI models of white matter. Front Phys. 2017;28:61.

39 Guglielmetti C, Veraart J, Roelant E, Mai Z, Daans J, Van Audekerke J, et al. Diffusion kurtosis imaging probes cortical alterations and white matter pathology following cuprizone induced demyelination and spontaneous remyelination. Neuroimage. 2016;125:363–377.

40 Jelescu IO, Zurek M, Winters KV, Veraart J, Rajaratnam A, Kim NS, et al. In vivo quantification of demyelination and recovery using compartment-specific diffusion MRI metrics validated by electron microscopy. Neuroimage. 2016;132:104–114.

41 Mollink J, Kleinnijenhuis M, Cappellen van Walsum AV, Sotiropoulos SN, Cottaar M, Mirfin C, et al. Evaluating fibre orientation dispersion in white matter: Comparison of diffusion MRI, histology and polarized light imaging. Neuroimage. 2017;157:561–574.

42 Salo RA, Belevich I, Jokitalo E, Gröhn O, Sierra A. Assessment of the structural complexity of diffusion MRI voxels using 3D electron microscopy in the rat brain. Neuroimage. 2021;225:117529.

43 Sepehrband F, Clark KA, Ullmann JF, Kurniawan ND, Leanage G, Reutens DC, et al. Brain tissue compartment density estimated using diffusion-weighted MRI yields tissue parameters consistent with histology. Hum Brain Mapp. 2015;36(9):3687–3702.

44 Veraart J, Fieremans E, Novikov DS. On the scaling behavior of water diffusion in human brain white matter. Neuroimage. 2019;185:379–387.

45 Coelho S, Baete SH, Lemberskiy G, Ades-Aron B, Barrol G, Veraart J, et al. Reproducibility of the Standard Model of diffusion in white matter on clinical MRI systems. Neuroimage. 2022;257:119290.

46 Zhang H, Schneider T, Wheeler-Kingshott CA, Alexander DC. NODDI: practical in vivo neurite orientation dispersion and density imaging of the human brain. Neuroimage. 2012;61(4):1000–1016.

47 Fieremans E, Jensen JH, Helpern JA. White matter characterization with diffusional kurtosis imaging. Neuroimage. 2011;58(1):177–188.

48 Diao Y, Jelescu I. Parameter estimation for WMTI-Watson model of white matter using encoder-decoder recurrent neural network. Magn Reson Med. 2023;89(3):1193–1206.

49 Jespersen SN, Olesen JL, Hansen B, Shemesh N. Diffusion time dependence of microstructural parameters in fixed spinal cord. Neuroimage. 2018;182:329–342.

50 Assaf Y, Freidlin RZ, Rohde GK, Basser PJ. New modeling and experimental framework to characterize hindered and restricted water diffusion in brain white matter. Magn Reson Med. 2004;52(5):965–978.

51 Novikov DS, Veraart J, Jelescu IO, Fieremans E. Rotationally-invariant mapping of scalar and orientational metrics of neuronal microstructure with diffusion MRI. Neuroimage. 2018;174:518–538.

52 Tristão Pereira C, Diao Y, Yin T, da Silva AR, Lanz B, Pierzchala K, et al. Synchronous nonmonotonic changes in functional connectivity and white matter integrity in a rat model of sporadic Alzheimer's disease. Neuroimage. 2021;225:117498.

53 Jelescu IO, Veraart J, Fieremans E, Novikov DS. Degeneracy in model parameter estimation for multi-compartmental diffusion in neuronal tissue. NMR Biomed. 2016;29(1):33–47.

54 Liao Y, Coelho S, Chen J, Ades-Aron B, Pang M, Osorio R, et al. Mapping tissue microstructure of brain white matter in vivo in health and disease using diffusion MRI. ArXiv [Preprint]. 2023:arXiv:2307.16386v2.

55 Edwards LJ, Pine KJ, Ellerbrock I, Weiskopf N, Mohammadi S. NODDI-DTI: Estimating Neurite Orientation and Dispersion Parameters from a Diffusion Tensor in Healthy White Matter. Front Neurosci. 2017;11:720.

56 Jelescu IO, de Skowronski A, Geffroy F, Palombo M, Novikov DS. Neurite Exchange Imaging (NEXI): A minimal model of diffusion in gray matter with inter-compartment water exchange. Neuroimage. 2022;256:119277.

57 Olesen JL, Østergaard L, Shemesh N, Jespersen SN. Diffusion time dependence, power-law scaling, and exchange in gray matter. Neuroimage. 2022;251:118976.

58 Lee HH, Olesen JL, Tian Q, Ramos Llorden G, Jespersen SN, Huang SY. Revealing diffusion time-dependence and exchange effect in the in vivo human brain gray matter by using high gradient diffusion MRI. Proc. Intl. Soc. Mag. Reson. Med. 2022. London, UK, p. 254.

59 Uhl Q, Pavan T, Molendowska M, Jones DK, Palombo M, Jelescu I. Quantifying human gray matter microstructure using Neurite Exchange Imaging (NEXI) and 300 mT/m gradients. Imaging Neuroscience. 2024;2:1–19.

60 Uhl Q, Pavan T, Feiweier T, Piredda GF, Jespersen SN, Jelescu I. NEXI for the quantification of human gray matter microstructure on a clinical MRI scanner. Proc. Intl. Soc. Mag. Reson. Med. 2024. Singapore.

61 Uhl Q, Pavan T, Feiweier T, Canales-Rodríguez EJ, Jelescu I. Optimizing The NEXI Acquisition Protocol For Quantifying Human Gray Matter Microstructure On A Clinical MRI Scanner Using Explainable AI. Proc. Intl. Soc. Mag. Reson. Med. 2023. Presented at the Annual Meeting of the ISMRM, Toronto, Canada, p. 948.
62 Williamson NH, Ravin R, Cai TX, Falgairolle M, O'Donovan MJ, Basser PJ. Water exchange rates measure active transport and homeostasis in neural tissue. PNAS Nexus. 2023;2(3):pgad056.
63 Hertanu A, Uhl Q, Pavan T, Lamy CM, Jelescu IO. Quantifying features of human gray matter microstructure postmortem using NeuriteExchange Imaging (NEXI) at ultra-high field. Proc. Intl. Soc. Mag. Reson. Med. 2023. Toronto, Canada.
64 Xu J, Does MD, Gore JC. Quantitative characterization of tissue microstructure with temporal diffusion spectroscopy. J Magn Reson. 2009;200(2):189–197.
65 Merboldt KD, Hänicke W, Bruhn H, Gyngell ML, Frahm J. Diffusion imaging of the human brain in vivo using high-speed STEAM MRI. Magn Reson Med. 1992;23(1):179–192.
66 Szczepankiewicz F, Sjölund J, Ståhlberg F, Lätt J, Nilsson M. Tensor-valued diffusion encoding for diffusional variance decomposition (DIVIDE): Technical feasibility in clinical MRI systems. PLoS One. 2019;14(3):e0214238.
67 Jiang X, Li H, Xie J, McKinley ET, Zhao P, Gore JC, et al. In vivo imaging of cancer cell size and cellularity using temporal diffusion spectroscopy. Magn Reson Med. 2017;78(1):156–164.
68 Reynaud O, Winters KV, Hoang DM, Wadghiri YZ, Novikov DS, Kim SG. Pulsed and oscillating gradient MRI for assessment of cell size and extracellular space (POMACE) in mouse gliomas. NMR Biomed. 2016 Oct;29(10):1350–1363.
69 Zhang H, Liu K, Ba R, Zhang Z, Zhang Y, Chen Y, et al. Histological and molecular classifications of pediatric glioma with time-dependent diffusion MRI-based microstructural mapping. Neuro Oncol. 2023;25(6):1146–1156.
70 Zhu A, Shih R, Huang RY, DeMarco JK, Bhushan C, Morris HD, et al. Revealing tumor microstructure with oscillating diffusion encoding MRI in pre-surgical and post-treatment glioma patients. Magn Reson Med. 2023;90(5):1789–1801.
71 Wu D, Jiang K, Li H, Zhang Z, Ba R, Zhang Y, et al. Time-Dependent Diffusion MRI for Quantitative Microstructural Mapping of Prostate Cancer. Radiology. 2022;303(3):578–587.
72 Szczepankiewicz F, van Westen D, Englund E, Westin CF, Ståhlberg F, Lätt J, et al. The link between diffusion MRI and tumor heterogeneity: Mapping cell eccentricity and density by diffusional variance decomposition (DIVIDE). Neuroimage. 2016;142:522–532.
73 Topgaard D. Multidimensional diffusion MRI. J Magn Reson. 2017;275:98–113.
74 Westin CF, Knutsson H, Pasternak O, Szczepankiewicz F, Özarslan E, van Westen D, et al. Q-space trajectory imaging for multidimensional diffusion MRI of the human brain. Neuroimage. 2016;135:345–362.
75 Szczepankiewicz F, Lasič S, van Westen D, Sundgren PC, Englund E, Westin CF, et al. Quantification of microscopic diffusion anisotropy disentangles effects of orientation dispersion from microstructure: applications in healthy volunteers and in brain tumors. Neuroimage. 2015;104:241–252.
76 Nilsson M, Englund E, Szczepankiewicz F, van Westen D, Sundgren PC. Imaging brain tumour microstructure. Neuroimage. 2018;182:232–250.
77 Nery F, Szczepankiewicz F, Kerkelä L, Hall MG, Kaden E, Gordon I, et al. In vivo demonstration of microscopic anisotropy in the human kidney using multidimensional diffusion MRI. Magn Reson Med. 2019;82(6):2160–2168.
78 Fokkinga E, Hernandez-Tamames JA, Ianus A, Nilsson M, Tax CMW, Perez-Lopez R, et al. Advanced Diffusion-Weighted MRI for Cancer Microstructure Assessment in Body Imaging, and Its Relationship With Histology. J Magn Reson Imaging. 2023. doi: 10.1002/jmri.29144. Epub ahead of print.
79 Reynaud O. Time-Dependent Diffusion MRI in Cancer: Tissue Modeling and Applications. Front. Phys. 2017;5. https://doi.org/10.3389/fphy.2017.00058
80 Lemberskiy G, Fieremans E, Veraart J, Deng FM, Rosenkrantz AB, Novikov DS. Characterization of prostate microstructure using water diffusion and NMR relaxation. Front Phys. 2018;6:91.
81 Lemberskiy G, Rosenkrantz AB, Veraart J, Taneja SS, Novikov DS, Fieremans E. Time-Dependent Diffusion in Prostate Cancer. Invest Radiol. 2017;52(7):405–411.
82 Lemberskiy G, Feiweier T, Gyftopoulos S, Axel L, Novikov DS, Fieremans E. Assessment of myofiber microstructure changes due to atrophy and recovery with time-dependent diffusion MRI. NMR Biomed. 2021;34(7):e4534.
83 McDowell AR, Feiweier T, Muntoni F, Hall MG, Clark CA. Clinically feasible diffusion MRI in muscle: Time dependence and initial findings in Duchenne muscular dystrophy. Magn Reson Med. 2021;86(6):3192–3200.
84 Piredda GF, Hilbert T, Granziera C, Bonnier G, Meuli R, Molinari F, et al. Quantitative brain relaxation atlases for personalized detection and characterization of brain pathology. Magn Reson Med. 2020;83(1):337–351.
85 Pavan T, Alemán-Gómez Y, Jenni R, Cleusix M, Alameda L, Do KQ, et al. Normative Modelling of White Matter Microstructure in Early Psychosis and Schizophrenia. Proc. Intl. Soc. Mag. Reson. Med. 2023. Toronto, Canada, p. 651.
86 Szczepankiewicz F, Lasič S, van Westen D, Sundgren PC, Englund E, Westin CF, et al. Quantification of microscopic diffusion anisotropy disentangles effects of orientation dispersion from microstructure: applications in healthy volunteers and in brain tumors. Neuroimage. 2015;104:241-252.

Contact

Ileana Jelescu, Ph.D.
Assistant Professor, SNSF Eccellenza, and ERC Starting Fellow
Microstructure Mapping Lab
Dept of Radiology, Lausanne University Hospital (CHUV) and University of Lausanne (UNIL)
Centre de Recherche en Radiologie PET3, CHUV
Rue du Bugnon 46
1011 Lausanne
Switzerland
Tel.: +41 21 314 6020
Ileana.Jelescu@chuv.ch